Journal of Multidisciplinary Engineering Science and Technology (JMEST)
ISSN: 2458-9403
Vol. 8 Issue 2, February - 2021

Adsorption of Lead (II) Ions from Aqueous Solutions Using Mangroves Roots (*Rhizophora Mucronata*) Charcoal-Carbon Nanotubes Nanocomposite

Fidelis Ngugi[1], Joel Mwangi[2], *Eric Njagi[3], Ochieng Ombaka[4]*

[1](Department of Physical Sciences, Chuka University, P.O. Box 109-60400, Chuka-Kenya)
[2](Department of Physical Sciences, Chuka University, P.O. Box 109-60400, Chuka-Kenya)
[3](Department of Physical Sciences, Chuka University, P.O. Box 109-60400, Chuka-Kenya)
[4](Department of Physical Sciences, Chuka University, P.O. Box 109-60400, Chuka-Kenya)

Abstract*—Providing clean and affordable water to meet human needs is a grand challenge of the 21st century. Worldwide, water supply struggles to keep up with the fast growing demand, which is exacerbated by population growth, global climate change, and water quality deterioration. Nanotechnology holds great potential in advancing water treatment to improve water treatment efficiency. In this study, Mangrove Roots Charcoal and Carbon Nanotubes (MRC-CNTs) nanocomposite was synthesized and utilized as a novel adsorbent for the removal of lead ions from aqueous solutions. The efficacy of MRC-CNT nanocomposites was investigated in batch mode which involved the effects of pH, temperature, concentration of the lead ions, adsorbent mass and contact time on adsorbates removal. Characterization of the adsorbent was carried out by Scanning Electron Microscopy (SEM) to observe the morphology of the adsorbent and surface area analysis and Energy Dispersive X-ray spectroscopy (EDX) to determine the elemental composition of the adsorbent. Adsorption isotherm models and adsorption kinetic studies were used for data analysis. It was observed that the removal efficiency of Pb (II) ions depended on pH of solution and the maximum efficiency was noticed at pH 7 with adsorption capacity of 3.629 mg/g which was calculated by the Freundlich isotherm model. Kinetic studies were well suited and found in good agreement with pseudo-second order. The results indicated that MRC-CNT nanocomposites would be a promising adsorbent for adsorption of Pb (II) ions from aqueous solutions.

Keywords—Nanotechnology, Adsorbent, Treatment and characterization.

1.0 INTRODUCTION

Water that is free of toxic chemicals and pathogens is crucial to human health, environment and to a variety of industrial processes [1]. Water on earth, is one of the most abundant natural resource, but only about 1% of that resource is available for human consumption [2] It is estimated that over 1.1 billion people lacking supply of adequate and reliable water due to increased rate of industrialization, population growth and global climate change. This problem is severe in developing nations and sub-Saharan African countries and Kenya is not an exceptional.

Lead, the metal considered in this study, is toxic nonessential heavy metal present in water and soil from different sources [3]. Lead is an element of concern because of its ability to bio-accumulate and its high toxicity even at low concentrations [4]. Generally, lead has been reported to cause renal dysfunction, hypertension, lung complications and bone lesions [5]. Further, exposure to lead may result in autism, psychosis, allergies, dyslexia, hyperactivity, paralysis and cancer with the latter being reported to be one of the leading causes of deaths in Kenya [6]. Considering these serious effects of lead, many scientists are making efforts to develop different adsorbents for the removal of Pb (II) ions from water and waste water.

Recent advances in manipulation of nanomaterials have facilitated the application of nanotechnology in water and wastewater treatment. Nanomaterials are defined as materials that at least one dimension is smaller than 100 nm [7]. At this scale, material exhibit unique physical and chemical properties over their bulky counterparts. For example, carbon nanotubes have higher density of active site per unit mass due to their large specific surface area. In addition, CNTs exhibit greater surface free energy resulting to enhanced surface reactivity [8].

In addition, CNTs possess tubular nanostructures with unique mechanical, physical, chemical and electrical properties, and possess large surface areas in addition to their layered structures [9]. Further, due to their hydrophobicity, they are usually oxidized with acids which causes shortening and thinning of tubes, and introduces polar functional groups such as –COOH and –OH on the tips or sidewalls of CNTs [10]. This processes helps in improving electrostatic interactions of CNTs for removal of organic and/or inorganic pollutants from water and waste water [3].

Therefore, the current study sought to synthesize and characterize functionalized mangrove roots charcoal-carbon nanotubes nanocomposites and explore its utilization as a novel adsorbent for the removal of lead ions from aqueous solution.

2.0MATERIALS AND METHODS

2.1Collection of mangrove roots and Functionalization of carbon nanotubes

Mangrove roots were collected from Dongo Kundu (Port area) in Mombasa County. The samples were washed with water, dried, ground and the powder carbonized using 1.0 M $ZnCl_2$ at 500 ^oC for 3h. The purified CNTs was functionalized by using a mixture of 6 M sulfuric and 6 M nitric acid in a volume ratio of 1: 3 at 80 ^oC for 12 h and the nanocomposite was prepared by dispersing 1.2 g of functionalized MWCNTs in 100 ml deionized water containing Mangrove Roots Charcoal (MRC) powder in the ratio of 1:3 by mass. The suspension was stirred for 2 h, filtered and then washed with deionized water until a neutral pH was obtained. The solid material was then dried in a vacuum oven at 80 ^oC overnight.

2.2Batch adsorption experiments

The influences of initial adsorbate concentration (0–50 mg/L), contact time (0–60 min), pH (2–10), adsorbent dosage (2–50 mg), speed (0-600 rpm) and temperature (25–75 ^oC) on the adsorption process were investigated. The batch mode adsorption experiments were conducted by bringing into contact the 50 mL of different Pb (II) solutions with a specified quantity of MRC-CNTs in a set of each 250 mL conical flasks. The concentration of residual Pb (II) ions was then determined by an Atomic Absorption Spectrophotometer (AAS, Buck Scientific 210VGP, USA). The Pb (II) removal efficiency, R (%) and equilibrium amount of Pb (II) adsorbed, qe, (mg/g), were calculated by Equations (1) and (2) below:

$$Q_e = \frac{(C_i - C_e)V}{m} \quad (1)$$

Where C_i and C_e are the initial and equilibrium concentrations (mg/L), *m* is the mass of the adsorbent (g) and *V* is the volume of the solution (mL).

$$\% \text{ Removal} = = \frac{C_0 - C_e}{C_0} \times 100 \quad (2)$$

2.3Adsorption isotherm models

The correlation between the amount of Pb (II) adsorbed onto MRC-CNTs and the equilibrium concentration of Pb (II) in the aqueous phase was evaluated using Langmuir, Freundlich isotherm, Dubin-Radushkevich and Temkin isotherms. The mathematical expression of Langmuir isotherm model is [4].

$$\frac{C_e}{q_e} = \frac{1}{Q_{\max} b} + \frac{1}{Q_{\max}} C_e \quad (3)$$

Where: q_e is the amount of solute adsorbed per unit weight of adsorbent (mg/g), C_e the equilibrium concentration of solute in the bulk solution (mgL^{-1}), Q_{max} the monolayer adsorption capacity (mgg^{-1}) and *b* is the Langmuir constant which reflects the binding strength between metal ions and adsorbent surface (Lmg^{-1}).

The mathematical expression of Freundlich isotherm model is [11].

$$Log\ q_e = K_F + \frac{1}{n} \log C_e \quad (4)$$

Where: q_e is the amount of solute adsorbed per unit weight of adsorbent (mgg^{-1}), C_e the equilibrium concentration of solute in the bulk solution (mgL^{-1}), K_F a constant indicative of the relative adsorption capacity of the adsorbent (mgg^{-1}) and the constant 1/*n* indicates the intensity of the adsorption. The D-R equation is given by:

$$\ln q_e = \ln q_m - K_{DR} \varepsilon^2 \quad (5)$$

where Ɛ (Polanyi potential) is equal to RT ln(1+1/Ce); q_m is the maximum adsorption capacity (mg /g) based on D–R isotherm and K is related to mean adsorption energy (E in kilojoule per mole). The Temkin isotherm model is based on the assumption that the free energy of adsorption is a function of the surface coverage and the linear form is presented as follows [12].

$$q_e = B \ln A + B \ln C_e \quad (6)$$

where A (L/mg) is the equilibrium binding constant, the constant B= RT/b_T (mg/g) is related to the heat of adsorption, R is the ideal gas constant (8.314 J/mol K), T (K) is the absolute temperature and b_T is the Temkin isotherm constant.

2.4Adsorption kinetic studies

The kinetic mechanism of the adsorption process was investigated by application of the pseudo-first order, pseudo-second order, intraparticle diffusion and liquid film diffusion model rate equations. Pseudo-first-order model is used to describe the reversibility of the equilibrium between solid and liquid phases [13] and is expressed by the equation shown below.

$$\log (q_e - q_t) = \log c_e - \frac{K_1}{2.303} t \quad (7)$$

Where: q_e and q_t are the amounts of heavy metal adsorbed (mg g^{-1}) at equilibrium and at the time (t min) and K_1 is the rate constant of the pseudo-first-order adsorption process (min^{-1}). Linear plots of log (q_e - q_t) versus t was used to predict the rate constant

(K_1) and adsorption at equilibrium (mg g^{-1}), which are obtained from the slope and intercept respectively. The pseudo-second-order equation assumes that the rate limiting step might be due to chemical adsorption [5]. According to this model, adsorbates can bind to two binding sites on the adsorbent surface and the equation can be expressed as shown below.

$$\frac{t}{q_t} = \frac{1}{K_2 q_e^{\,2}} + \frac{1}{q_e} t \qquad (8)$$

Where: K_2 is the rate constant of the pseudo-second-order adsorption ($gmg^{-1}min^{-1}$). If the adsorption kinetics obeys the pseudo-second-order model, a linear plot of t/q_t versus t can be observed. The intraparticle diffusion equation is given as follows [14]

$$q_t = K_d\, t^{\frac{1}{2}} + C \qquad (9)$$

Where K_d (mg g^{-1} $min^{-1/2}$) is the intraparticle diffusion rate constant and C represents the intercept and is related to the thickness of the boundary layer. When the transport of the adsorbate from the liquid phase to the solid phase boundary plays the most significant role in adsorption, then the liquid film diffusion model can be applied [15].

$$\ln(1 - F) = -K_{fd} + Y \qquad (10)$$

Where $F = \frac{q_t}{q_e}$ is the fractional attainment of equilibrium, K_{fd} (mg/g min) is the film diffusion adsorption rate constant and Y is the intercept. A linear plot of ln (1− F) versus t suggests that the kinetics of adsorption involves a film diffusion mechanism. Furthermore, if the plot is linear with (Y = 0) then film diffusion is the sole rate controlling mechanism.

3.0 RESULTS AND DISCUSSIONS

3.1Effect of MRC -CNTs dose on adsorption of lead (II) ions

It is important to determine the optimum dosage of MRC-CNTs on Pb^{2+} ions adsorption system. Figure 25 shows the influence of the adsorbent dosage on percentage adsorption of Pb^{2+} from aqueous solution.

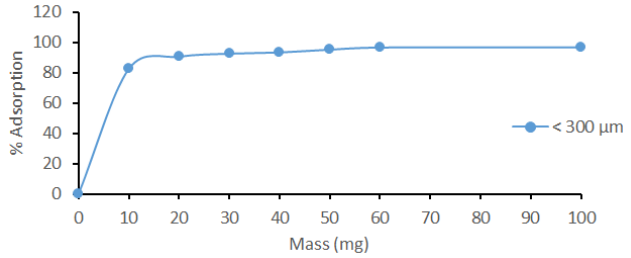

Figure 1: Effect of MRC-CNTs weight on % adsorption of 50 ppm of Pb^{2+} ions.

The percentage removal of Pb^{2+} from the solution increased with the dosage, until a dosage of 50 mg after which the amount of Pb^{2+}adsorbed remained constant. The rapid uptake of metal ions for the first 10 mg as shown in Figure 25 was attributed to the increased availability of exchange sites or the increase in the surface area that featured large number of adsorption sites. The insignificant adsorption from 50 to 100 mg may be due to the overlapping or aggregation of the adsorbent particles, which leads to a decrease in the available adsorbent surface area and an increase in the diffusional resistances [8].

3.2Effect of initial concentration of adsorbates on adsorption of lead (II) ions

To study the effect of Pb (II) removal as a function of initial metal ion concentration the initial metal ion concentration was varied from 10 to 100 mg L^{-1}, while contact time was 30 min at a constant shaking speed of 300 rpm.

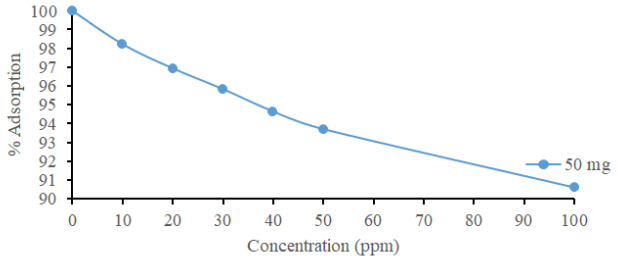

Figure 2:Effect of Initial Pb (II) ions Concentration on Adsorption by 50 mg MRC-CNTs Nanocomposite

It is evident from Figure 26 that increase in initial concentration of Pb^{2+} ions from 10 to 100 mg L^{-1} resulted in decrease in % adsorption from 98.22% to 90.61% respectively. This was because at high initial concentrations of adsorbate, the number of moles of Pb^{2+} ions available to the surface area were high, so functional adsorption became dependent on the initial concentration. The decrease in the % adsorption could also be attributed to saturation of the adsorption sites or lack of sufficient surface area to accommodate much more metal ions available in solution [3]. At lower concentrations, all the Pb^{2+} could interact with the binding sites and thus a higher % adsorption than at higher Pb^{2+} concentrations.

3.3 Effect of contact Time on Adsorption of Lead (II) ions

The experiment was conducted by varying the contact time from 0 to 60 minutes at 5 minutes' interval.

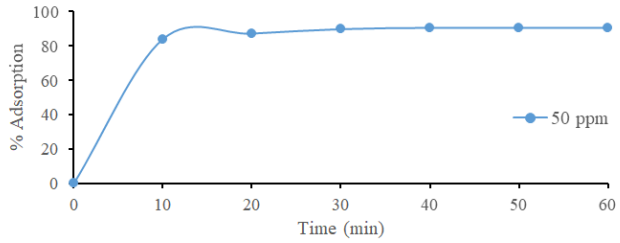

Figure 3:Effect of Contact Time on Adsorption of Pb^{2+} ions onto 50 mg of MRC-CNTs Nanocomposite

From Figure 27, it is clear that the rate of removal of Pb (II) ions was rapid for the first 10 min where there was more than 80% removal of lead within that time. Equilibrium was established after 30 min and thereafter no significant increase in % removal with increase in contact time was observed. This observation was probably due to the larger surface area of the adsorbent being available at the beginning of adsorption process [8]. After the formation of one molecule thick layer of metal ion on the adsorbent, the adsorbent capacity got exhausted, and then the uptake rate was controlled by the rate at which the adsorbate was transported from the exterior to the interior sites of the adsorbent [7]

3.4Effect of Temperature on Adsorption of Pb (II) ions

To determine the effect of temperature on the adsorption of Pb (II) ions, experiments were conducted at temperature of 25, 35, 45, 55, 65 and 75 ^{o}C.

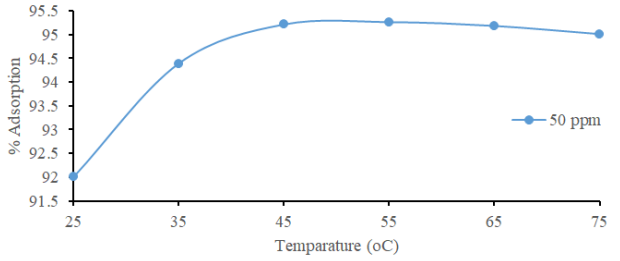

Figure 4:The Effect of Temperature on Adsorption of Pb^{2+} ions by 50 mg MRC-CNTs Nanocomposite

The degree of adsorption increased with increase in temperature, indicating that adsorption process was controlled by an endothermic process [4]. Increased adsorption with rise in temperature up to 45 ^{o}C could be attributed to increase in the number of active surface sites available for adsorption, increase in kinetic energy of lead ions, increased porosity and the pore volume of the adsorbent and decrease in the viscosity of the solution [16].

3.5 Effect of pH on Adsorption of Pb (II) ions by MRC-CNTs Nanocomposite

Hydrogen ions concentration is one of the important factors that influence the adsorption behavior of metal ions in aqueous solutions [17]. It affects the solubility of metal ions in solution, replaces some of the positive ions found in active sites and affects the degree of ionization of the adsorbate during the process of adsorption [5]. Thus the effect of pH on the removal efficiency of Pb (II) was studied at different pH ranging from 2.0 to 10.0. The results are as shown in Figure 30.

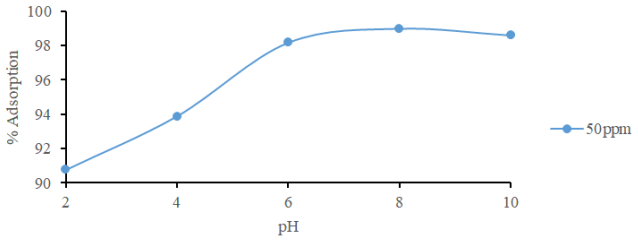

Figure 5:Effect of pH on the % Adsorption of 50ppm Pb^{2+} ions by 50 mg of MRC-CNTs

It is clear from the graph that the removal efficiency of Pb^{2+} increased as the pH values increased from 2 (90.74%) to 8 (98.98%) and decreased insignificantly at pH 10 (98.59%). At low pH values, the protonation of the functional groups present on the adsorbent surface easily takes place, and thereby restrict the approach of positively charged ions to the surface of the adsorbent resulting in low adsorption of Pb (II) in acidic solution. With decrease in acidity of the solution, the functional groups on the adsorbent surface become de-protonated resulting in an increase in the negative charge density on the adsorbent surface and facilitate the binding of lead cations. The increase in lead removal capacity at higher pH may also be attributed to the reduction of H^{+} ions which compete with metal cations at lower pH for appropriate sites on the adsorbent surface. However, with increasing pH, this competition weakens and lead cations replace H^{+} ions bound to the adsorbent surface resulting in increased Pb (II) ions uptake. The slight reduction in removal observed at pH > 8 was attributed to precipitation of Pb (II) ions forming lead hydroxide which competed with lead ions.

3.6Adsorption Isotherm Studies for Pb (II) ions onto MRC-CNTs

In the present study, Langmuir, Freundlich, Dubinin- Radushkevich and Temkin isotherm models were utilized to explain the experimental data as given in Figures 31, 32, 33, and 34.

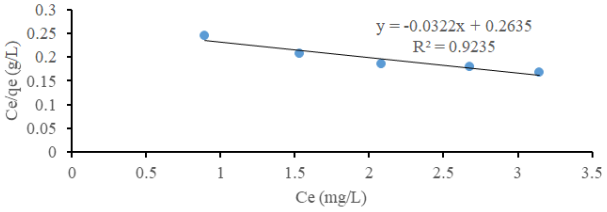

Figure 6: Langmuir Isotherm for Pb (II) ions Adsorption onto 50 mg g MRC-CNTs Nanocomposite

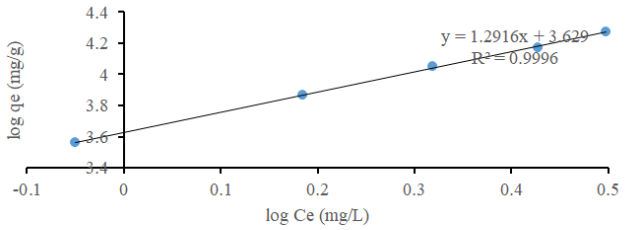

Figure 7:Freundlich isotherm for Adsorption of Pb (II) ions onto 50 mg MRC-CNTs Nanocomposite.

Table 1:Langmuir, Freundlich, Dubin-Radushkevich and Temkin isotherm models Parameters for Pb (II) ions Adsorbed onto 50 mg MRC-CNTs Nanocomposite

Langmuir			**Freundlich**		
Q_{max}(mg g^{-1})	***b*(L mg^{-1})**	**R^2**	**K_F(mg g^{-1})**	n	R^2
-31.0559	0.1222	0.9235	3.629	0.7742	0.9996
Dubin- Radushkevich			**Temkin**		
Q_m (mg g-1)	**E ($Kjmol^{-1}$)**	**R^2**	**A (L mg^{-1})**	B	R^2
18.1941	10.0	0.9115	1.386	11.63	0.9485

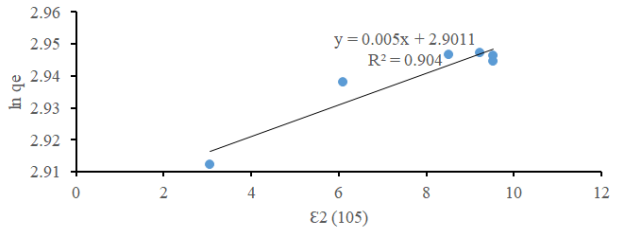

Figure 8: Dubin- Radushkevich isotherm for Pb (II) ions Adsorption onto 50 mg g MRC-CNTs Nanocomposite

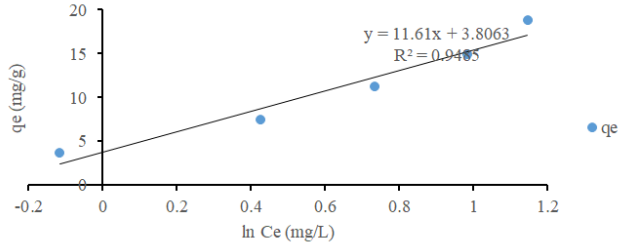

Figure 9: Temkin isotherm for Pb (II) ions Adsorption onto 50 mg g MRC-CNTs Nanocomposite

The best fit equilibrium model was determined based on the linear regression correlation coefficient (R^2) and for that case Freundlich isotherm model was selected since it had the highest correlation coefficient of 0.9996 with adsorption capacity of 3.629 mg g^{-1}. The results were comparable to that of the study conducted by [17] on nanomaterials for the removal of heavy metals from wastewater.

3.7Adsorption Kinetics of Pb (II) ions

The kinetic studies of Pb (II) adsorption on MRC-CNTs nanocomposite was carried out using the pseudo-first-order, pseudo-second–order, liquid film diffusion and intra-particle diffusion models on experimental data. The results are shown in figures 35 to 40.

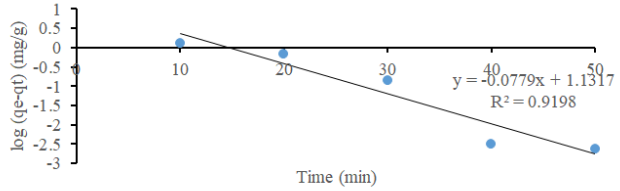

Figure 10:Pseudo-First-Order Plot of Pb (II) Adsorption onto 50 mg MRC-CNTs Nanocomposite for 50 ppm of Pb (II) ions.

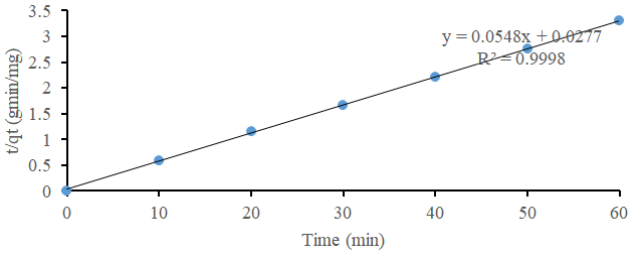

Figure 11:Pseudo-Second-Order Plots for Adsorption of 50 ppm Pb (II) ions onto 50 mg MRC-CNTs Nanocomposite

Table 2:Pseudo-First-Order, Pseudo–Second-Order, intraparticle and liquid film diffusion Rate Constants for Adsorption of Pb (II) ions on 50 mg MRC-CNTs

Pseudo-first-order				Pseudo-second -order		
Pb (ppm)	**$Q_{e(mg/g)}$**	**Constant (min^{-1})**	**R^2**	**Q_e(mg/g)**	**Constant (g/mg/min)**	**R^2**
50	26.89	0.1794	0.9198	18.2481	0.1084	0.9998
Intraparticle diffusion				**Liquid film Diffusion**		
Pb (ppm	**C(mg g^{-1})**	**K_d(mg g^{-1} $min^{-1/2}$)**	**R^2**	**Intercept**	***K_{fd}*(mg/gmin)**	**R^2**
50	16.106	0.2893	0.8488	0.2906	0.1793	0.9198

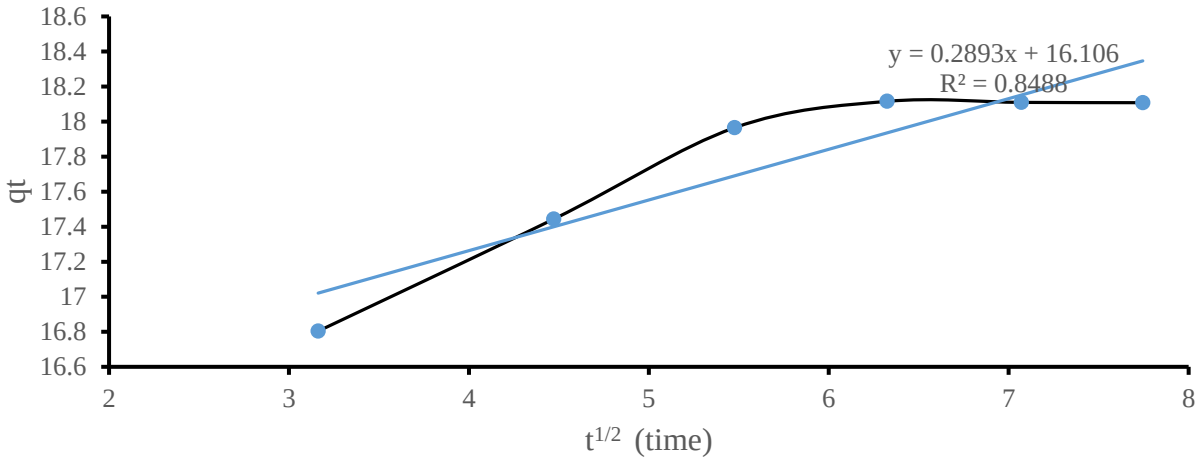

Figure 12:Intra-particle Plots for Adsorption of 50 ppm Pb (II) ions onto 50 mg MRC-CNTs Nanocomposite

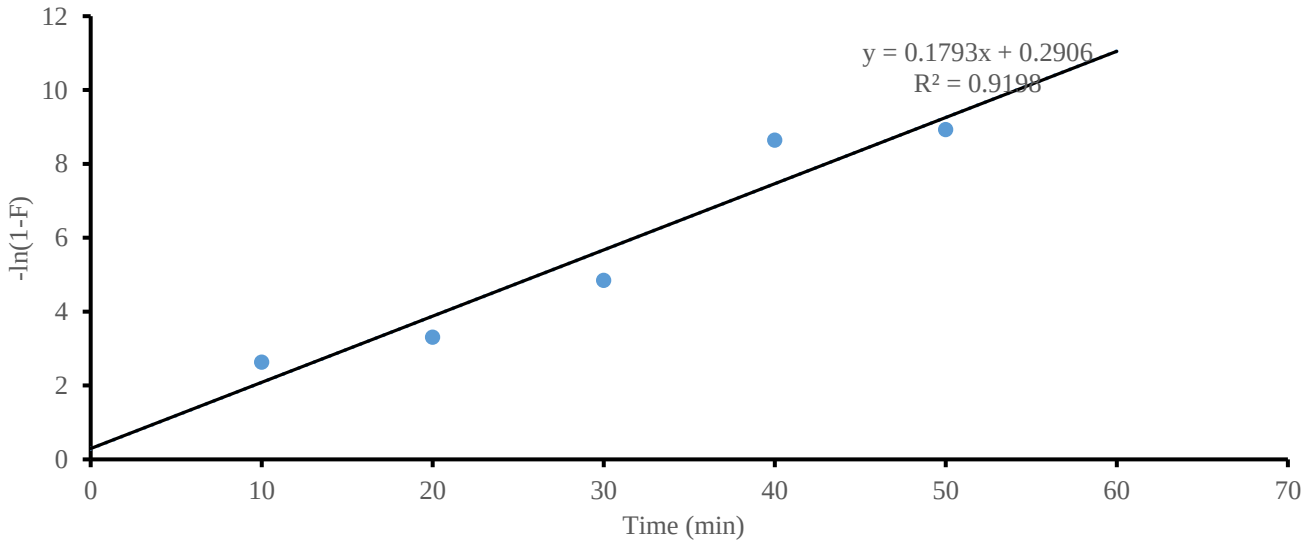

Figure 13:Liquid film Plot for Adsorption of 50 ppm Pb (II) ions onto 50 mg MRC-CNTs Nanocomposite

These findings imply that the mechanism of adsorption of Pb (II) ion on the MRC-CNT follows the pseudo-second-order kinetics, indicating that the rate-limiting step was a chemical adsorption process between the metal ion and MRC-CNTs nanocomposite.

4.0 Conclusions

In this work, the ability of MRC-CNTs to remove Pb (II) ions from aqueous solution was investigated. It was found that the prepared MRC-CNTs acted as an effective adsorbent for the removal of Pb (II) ions with

adsorption capacity of 3.629 mg/g which was calculated by the Freundlich isotherm model.

4.1Recommendations

The following recommendations were made for future study:

i. A pilot-scale column with the developed adsorbent can be conducted for real wastewater.
ii. A suitable modification method for preparing adsorbents can be considered to obtain maximum removal of heavy metals and dyes.
iii. The performance of removal of other heavy metals along with other organic pollutants like pesticides and nitrates can be evaluated by using the developed adsorbents.

References

[1]Etorki, A. M. (2014) Removal of some Heavy Metals from Wastewater by using of Fava Beans. *American Journal of Analytical Chemistry* **5**, 225-

[2]Anjum, M., Miandad, R., Waqas, W., Gehany, F., Barakat, M. A. (2016) Remediation of wastewater using various nano-materials, *Arabian Journal of Chemistry*. 234.

[3]Nyairo, W. N. Eker, Y. R., Kowenje, C. Akin, I., Bingol, H., Tor, A. and Ongeri, D. M., (2018), Efficientadsorption of lead (II) and copper (II) from aqueous phase using oxidized multiwalled carbonnanotubes/polypyrrole composite, Separation Science and Technology, 1520-1527

[4]Aravind, J., Shanmugaprakash, M., Sangeetha, H. S., Lenin C. and Kanmani, P. (2013) Pigeon Pea (*Cajanuscajan*) Pod as a Novel Eco-Friendly Biosorbent: A Study on Equilibrium and Kinetics of Ni (II) Biosorption. *International Journal of Industrial Chemistry* 4, 1-25.

[5]Amboga, D. A., Onyari, J. M., Shiundu, P. M. and Gichuki, J. W. (2014) Equilibrium and Kinetics Studies for the Biosorption of Aqueous Cd (II) ions onto *Eichhornia crassipes* Biomass. *Journal of Applied Chemistry* 7 (1), 29-37.

[6]Mataka, L. M., Henry, M. T., Masamba, R. L. and Sajidu, S. M. (2006) Lead Remediation of Contaminated Water using *Moringa stenopetala* and *Moringa oleifera* Seed Powder. *International Journal of Environmental Science and Technology* 3 (2); 131-139.

[7]Qu, X., Pedro J.J., Li, Q. (2013) Applications of nanotechnology in water and wastewater treatment, *Water Research*, 47(12,) 3931-3946

[8]Esmaeili, A., Eslami, H. (2019) Efficient removal of Pb(II) and Zn(II) ions from aqueous solutions by adsorption onto a native natural bentonite, *Journal of applied chemistry*, 6, 1979–1985

[9]Hamza, A. A, Martincigh, S. B., Ngila J. C. and Nyamori, O.C. (2013) Adsorption Studies of Aqueous Pb(II) Ions onto a Sugarcane Bagasse/Multiwalled Carbon Nanotubes Composites. *Physics and Chemistry of the Earth* 66, 157 – 166.

[10]Oyetade, A. O., Nyamori, O. V., Martincigh, S. B. and Jonnalagadda, B. S. (2016) Nitrogen Functionalized Carbon Nanotubes as a Novel Adsorbent for the Removal of Cu (II) from Aqueous Solution. *The Royal Society of Chemistry.* 6, 2731-2745.

[11]Hameed, B. H and Ahmad, A. A and (2009) Reduction of COD and Color of Dyeing Effluent from Cotton Textile Mill by Adsorption onto Bamboo-based Activated Carbon. *Journal of Hazardous Materials* 172, 1538–1543

[12]Akpomie, K. G. and Dawodu, A. F. (2015) Treatment of an Automobile Effluent from Heavy Metals Contamination by an Ecofriendly Montmorillonite. *Journal of Advanced Research 6,* 1000-1013.

[13]Vijaya, K. and Yun, V. S. (2008) Bacterial Biosorbents and Biosorption. *Biotechnology Advances* 26, 266-291.

[14]Kooh, R. R. M., Dahri, K. M., and Lim, B. L. L. (2016) The Removal of Rhodamine B dye from Aqueous Solutions using *Casuarinaequisetifolia* Needles as Adsorbent. *Cogent Environmental Science* 2, 1-14.

[15]Taffarel S. R. and Rubio J. (2009) On the Removal of Mn Ions by Adsorption onto Natural and Activated Chilean Zeolites. *Journal of Mineral and Engineering* 22, 336-343.

[16]Hamzat, W. A., Abdulkareem, A. S., Bankole, M. T., Tijani, J.O. Kovo, A. S. Abubakre, O. K. (2019) Adsorption studies on the treatment of battery wastewater by purified carbon nanotubes (P-CNTs) and polyethylene glycol carbon nanotubes (PEG-CNTs), *Journal of Environmental Science and Health*, Part A, 54:9, 827-839

[17]He, Y., Wu, P., Xiao, W., Li, G., Yi, J. (2019) Efficient removal of Pb(II) from aqueous solution by a novel ion imprinted magnetic biosorbent: Adsorption kinetics and mechanisms, Journal of Applied Chemistry 4(3) pp19

.

Kaushal, A. and Singh, S. K., (2017), Removal of heavy metals by nanoadsorbents: A review *Journal of Environment and Biotechnology Research*, 6, (1), 96-104